Applied Surface Science 546 (2021) 149114

Contents lists available at ScienceDirect

Applied Surface Science

journal homepage: www.elsevier.com/locate/apsusc

Full Length Article

Robust and impermeable metal shell microcapsules for one-component self-healing coatings

Dawei Sun [a], Zheng Yan [a], Lan Mingzhang [a], Wang Ziming [a], Cui Suping [a,*], Yang Jinglei [b,*]

[a] College of Materials Science and Engineering, Beijing University of Technology, Beijing 100124, China
[b] Department of Mechanical and Aerospace Engineering, Hong Kong University of Science and Technology, Hong Kong Special Administrative Region

ARTICLE INFO

Keywords:
Metal shell
One component self-healing
Anticorrosion coatings
Isocyanates

ABSTRACT

Metal shell microcapsules containing liquid 4,4′-bis-methylene cyclohexane diisocyanate (HMDI) were successfully synthesized by plating chemically a layer of Ni-P alloy on microcapsules surfaces. The metal shell occupied around 66.0 wt% of final microcapsules, providing great potential to improve microcapsules robustness. Final microcapsules with diameters of 184.3 ± 41.7 μm had a core fraction of 22.4 ± 0.6 wt%. The final microcapsule shells with a total thickness of 7.4 ± 0.4 μm was a three-layered structure, which comprised of an outer-layered Ni-P shell with a thickness of 5.5 ± 0.2 μm, a medium-layered PUF shell with a thickness of 369.0 ± 21.0 nm, and an inner-layered polyurea shell with a thickness of 1.7 ± 0.2 μm. More interestingly, final microcapsules remained stable core fraction and morphologies in most regular solvents including low polar organic solvents, high polar organic solvents, and water. The shell strength of final microcapsules was 28.5 ± 10.3 MPa, comparing with 6.6 ± 2.5 MPa of polymer shells. Moreover, the modulus of epoxy composites was stable relatively with microcapsules concentrations. Scratched self-healing epoxy coatings showed satisfactory anticorrosion performance in salty water (1 M).

1. Introduction

The corrosion of steel rebar shortened the durability of concrete structures and brought great economic loss and human safety concerns annually [1–3]. Although a passive layer was formed on the surfaces of steel rebars in the alkaline environments (pH ~ 13) of concretes, it was vulnerable to surrounding chloride ions and lost barrier effects along with anticorrosion capabilities [4]. Besides strength compromise, the volume expansion of corroded steel rebar caused unavoidable cracking and spalling of concretes. The organic coating was one of the most popular anticorrosion techniques for steel rebar due to its good barrier effects [5], efficiency, economy and feasibility [2]. However, organic coatings were vulnerable to physical attacks from sands, stress, or abrasion, resulting in the re-exposure and more serious corrosion of steel bars.

The self-healing technique was an efficient method to retard the corrosion of steel rebars by healing automatically damaged protective coatings. Especially, microcapsule as a kind of newly developed technique showed great potentials to fabricate self-healing anticorrosion coatings of steel rebars [6]. Microcapsules in coatings were broken by the propagation of cracks and released healing agents to seal cracks. Until now, epoxy resin [7], organic silicone [6], and dicyclopentadiene (DCPD) [8] were encased successfully and showed satisfying self-healing functions in coatings. However, such healing agents needed catalyst or cure agents as the second component to finish the healing process. The correct stoichiometric ratio of both components within cracks was mostly uncontrolled, resulting in unsatisfactory self-healing performance. To conquer this shortage, one component self-healing system was proposed by applying isocyanate [9], 1H, 1H, 2H, 2H-perflurooctyltriethoxysilane (POTs) [10], linseed oil [11], or light cure resin [12] as healing agents, which were solidified under the action of environmental water, oxygen or UV light. It was worth noting that isocyanates microcapsules presented outstanding self-healing anticorrosion performance, but survived short-timely in such concrete environments as moist, mechanical abrasion, or organic solvents [9], due to the weak robustness and impermeability of polymer shells. However, complex and harsh environments of cement-based materials required isocyanates microcapsules to possess high robustness and outstanding impermeability [13] for a longer service life of organic coatings.

Various methods were provided to adjust the robustness and

* Corresponding authors.
E-mail addresses: cuisuping@bjut.edu.cn (C. Suping), maeyang@ust.hk (Y. Jinglei).

https://doi.org/10.1016/j.apsusc.2021.149114
Received 21 October 2020; Received in revised form 30 December 2020; Accepted 21 January 2021
Available online 27 January 2021

impermeability of microcapsule shells. Wang et al. [14] used oxygen plasma-treated carbon nanotubes as fillers to improve the micro-mechanical behavior of polyurea shells. Caruso et al. [15] boosted shell strength by increasing thickness, which was achieved by combining interfacial and in situ encapsulation methods. Zhang et al. [16] loaded healing agents in hollow glass bubbles with higher mechanical strength than polymer shells. Sun et al. [17,18] applied successfully double-layer shell structures to obtain stable microcapsules in both water and organic solvents. However, the robustness and impermeability of microcapsules still remained long-term challenging. In recent years, metal shells were proposed gradually to improve the stability of microcapsules in harsh conditions, due to their higher strength and better impermeability. Traditional vacuum evaporation deposition method merely fabricated a layer of a thin metal membrane with thickness in nano-scale, which hardly withstood external collision and solvents extraction [19]. Chemical plating techniques were permissible to fabricate thick metal shells, and were applied successfully on such solid surfaces as powders [20] and natural silk [21]. Besides, Patchan et al. [22] tried to coat a layer of Nickel shell on the surface of microcapsules. Sun et al. [23] fabricated a layer of Nickel shell with an adjustable thickness on the surface of such liquid droplets as epoxy resin, DCPD, and liquid wax. Encasing isocyanates within metal shells had great potentials to boost the mechanical properties and the chemical stability of microcapsules, obtaining self-healing anticorrosion coatings of steel rebars with longer service life and wide applications.

In this paper, we fabricated successfully a layer of Nickel-P shell on the surface of polymer microcapsules with 4,4′-methylenebis(cyclohexyl isocyanate) (HMDI) as core material through a chemical plating technique. Final microcapsules presented outstanding stability in water and high polar organic solvents. Moreover, final self-healing coatings possessed high modulus and satisfying self-healing anticorrosion performance.

2. Experiments

2.1. Chemicals

4,4′-diphenylmethane diisocyanate (MDI) prepolymer (Suprasec 2644) was obtained from Huntsman. 4,4′-methylenebis(cyclohexyl isocyanate) (HMDI), gum Arabic, ethylene maleic anhydride (EMA), ammonium chloride (NH_4Cl), tetraethylenepentamine (TEPA), hexane, xylene, ethyl acetate, acetone, ethanol, hydrochloric acid solution (HCl, 0.1 M), potassium bromide (KBr), sodium hydroxide (NaOH), sodium chloride (NaCl), palladium chloride, stannous chloride, Nickel sulfate, sodium hypophosphite monohydrate, sodium acetate, malic acid, lactic acid, thiourea, Tergitol (NP-9) and triethanolamine were purchased from Sigma-Aldrich. Epolam 5015 and hardener 5014 used as epoxy coating were supplied by Axson. All chemicals in this study were used as received without further purification.

2.2. Synthesis of metal shell microcapsules

The synthesis of metal shell microcapsules was divided into two steps. The first step was to synthesize microcapsules with polymer shells. The second step was to fabricate a layer of metal shell on polymer microcapsule surfaces.

2.2.1. Synthesis of polymer microcapsules

The synthesis of polymer microcapsules followed our previous methods [18]. The polymer microcapsules were prepared via interfacial polymerization in an oil-in-water emulsion system, followed by in situ encapsulation method. Firstly, the water phase, 30 ml of deionized (DI) water containing 2.5 wt% of gum Arabic was heated up to 30 °C in a 250 ml beaker, which was placed in a temperature controlled water bath located on a programmable hotplate.

Later, the uniform oil phase containing 0.5 g of Suprasec 2644 and 4.5 g of HMDI was emulsified into micro-droplets in the surfactant aqueous solution under a certain agitation rate (Caframo, model: BDC6015). After the emulsion system was stabilized for 45 min at 30 °C, 18.0 g of TEPA aqueous solution (30 wt%) was added to initiate the interfacial polymerization. Meantime, the system temperature was raised to 65 °C. After reaction for 30 min at the designated temperature, the microcapsule slurry was rinsed with DI water 3–4 times for the next operations.

Subsequently, the in situ encapsulation method was applied to fabricate polymer microcapsules. Urea-formaldehyde prepolymer was firstly synthesized by polymerizing 6.33 g of formaldehyde aqueous solutions (37 wt%) with 2.5 g of urea at pH value of 7.5–8.5 and temperature of 70 °C for 1 h. Then the urea–formaldehyde prepolymer and 1.5 g of resorcinol were dissolved in 60 ml of EMA aqueous solutions (1.25 wt%) as prepolymer aqueous solutions. Subsequently, the microcapsules slurry was added in prepolymer aqueous solutions with final pH value of 3.0. The mixture was then allowed to stabilize for 50 min at room temperature followed by elevating the temperature to 55 °C. After 2 h, the final microcapsules slurry was rinsed with DI water several times, and then air-dried 12 h to obtain polymer microcapsules.

2.2.2. Fabrication of metal shell microcapsules

The metal shell microcapsules were synthesized by plating a layer of Nickel-P alloy covering polymer microcapsules.

Firstly, the Pd particles were deposited on the surfaces of polymer microcapsules. 0.025 g of $PdCl_2$ was dissolved in 5 ml of concentrated HCl solution (36 wt%) in a 50 ml glass beaker, which was suspended in a water bath with a temperature of 30 °C on a magnetic stirring apparatus. After the complete dissolve of $PdCl_2$ in concentrated HCl solutions, 0.0635 g of $SnCl_2$ was introduced and allowed to react for 10 min with the formation of suspended Pd particles solutions, which was then added into polymer microcapsules slurry at 30 °C under agitation rate of 200 RPM. After 10 min, the polymer microcapsules with Pd on the surface were rinsed several times for the future plating process.

Subsequently, a layer of Nickel-P alloy was plated on the surface of polymer microcapsules. Plating solutions were prepared by mixing uniformly 3.0 g of nickel sulfate, 3.0 g of sodium hypophosphite monohydrate, 2.0 g of sodium acetate, 0.4 g of malic acid, 2.0 ml of lactic acid, 1 droplet of Tergitol, and 10 droplets of thiourea solutions (0.01 g thiourea in 100 ml DI water). The pH value of the plating solution was adjusted to 5.5 with triethanolamine and then heated to 70 °C. Subsequently, polymer microcapsules with catalyst were added into plating solutions and allowed to proceed for another 60 min. Finally, the metal shell microcapsules were rinsed and washed for future characterization after air drying for 12 h.

2.3. Characterization of microcapsules

The morphology, size, and shell thickness of final microcapsules were observed through a scanning electron microscope (FESEM, Joel, Model: JSM-7600F). The size distributions of the microcapsules were derived from the statistic of at least 150 individuals using ImageJ in SEM images. Microcapsules were mounted on conductive tape and some of them were ruptured with a razor blade to observe the core-shell structures.

Spectrophotometer (Varian 3100) was applied to obtain FTIR spectra curves of pure HMDI and core material. The range of the applied spectrum was within 1000–4000 cm^{-1}. The composition of metal shells was determined through Energy Dispersive X-Ray Spectroscopy (EDX).

The core fractions of metal shell microcapsules were derived by titrating NCO (active functional groups of isocyanates and one HMDI molecule contained two NCO functional groups) contents of crushed microcapsules and then converted into the weight of HMDI core, which possessed stoichiometric relation with NCO functional groups. A certain amount of microcapsules were crushed firstly with two pieces of clean glass slides. The broken microcapsules were then flushed into a glass

beaker with massive acetone. Subsequently, the NCO content in acetone solutions was titrated according to ASTM D2572-97 and then converted into the weight of HMDI. The calculation method of HMDI was shown as the following:

$$m_{HMDI} = 262.35 \times 0.5 \times n_{NCO} = 131.18 \times \frac{(v_{blank} - V) \times c_{HCl}}{2000} \quad (1)$$

$$core \quad fraction \quad (wt\%) = \frac{m_{HMDI}}{m_{microcapsules}} \times 100\% \quad (2)$$

where m_{HMDI}(g) was the weight of the HMDI core. 262.35 was the equivalent weight of the HMDI. V_{blank} (ml) and V (ml) were the volumes of the standard HCl (0.1 M) aqueous solution consumed by the blank experiment and titration sample, respectively. c_{HCl} was the normality of standard HCl (0.1 M) aqueous solution, *core fraction* (wt%) was the core fraction of microcapsules, and $m_{microcapsules}$(g) were the masses of samples.

The thermal stability of the final microcapsules was characterized through TGA (Q500) tests. 10–20 mg of microcapsules, shell material, core material, and pure HMDI were heated from room temperature to 600 °C at a rate of 10 °C/min in a Nitrogen atmosphere. The weight loss curves of samples were obtained as a function of temperatures. The beginning decomposition temperature of samples was determined as the temperature when samples lost weight of 5.0 wt%.

2.4. Stability tests of microcapsules

The stability of metal shell microcapsules in water and organic solvents was tested by immersing metal shell microcapsules in solvents for certain durations and then characterized in terms of residual core fractions and morphologies.

2.4.1. Stability of microcapsules in water

A certain amount of metal shell microcapsules was soaked in ambient water (ambient temperature: 25 °C) at a concentration of 5 wt%. After designated durations (10 days and 20 days), the soaked microcapsules were rinsed with DI water for subsequent core fraction determination after air dried for 12 h.

2.4.2. Stability of microcapsules in organic solvents

Organic solvents including low-polar (hexane, xylene), medium polar (ethyl acetate), and polar (acetone) organic solvents were applied to measure the stability of metal shell microcapsules. The microcapsules were immersed in organic solvents for certain durations at designated concentrations. Subsequently, the microcapsules were filtrated and washed, followed by characterization in terms of residual core fractions and morphology after air-dried for 12 h.

2.5. Mechanical properties investigations

The mechanical property investigation was divided into two parts. The first part was to test the micro-compression strength of individual microcapsules. And the second part was to test the compression strength of epoxy composites containing microcapsules.

2.5.1. Mechanical property of single microcapsule

The compression strength of a microcapsule was measured through published microsphere compression experiments [24]. The load was recorded by a load cell (FUTEK) with a maximum load of 0.5 N and the applied loading rate for the stepper actuator (Physik Insturmente M-230S), which was controlled by a computer, was 2 μm/s. In addition, the diameter of the microcapsules was measured by the images taken prior to the test. The shell strength was calculated according to the following equation.

$$\delta_{max} = \frac{P_{max}}{\pi\left[\left(\frac{D_0}{2}\right)^2 - \left(\frac{D_i}{2}\right)^2\right]} \quad (3)$$

where $\sigma_{max}$was the normalized maximum strength; P_{max} was the maximum load; D_0 was the outer diameter of microcapsules; D_i was the inner diameter of microcapsules.

2.5.2. Mechanical properties of epoxy composites

The influence of microcapsules on matrix strength was characterized through the compression strength of epoxy composite containing microcapsules at different concentrations. In comparison, the compression strength of pure epoxy samples was tested. Compression specimens were fabricated and tested according to ASTM-D695. The epoxy resin was precured for 3 h at room temperature followed by the addition of metal shell microcapsules and then degassing in a vacuum to remove trapped bubbles. Subsequently, the mixtures were added to silicone rubber mold for molding. Instron machine (Instron 5500R) was applied to conduct the compression test with a loading speed of 1 mm/min.

2.6. Preparation and test of anticorrosion coatings

The metal shell microcapsules were dispersed in epoxy resin (Epolam 5015 and hardener 5014) at a concentration of 10 v% to fabricate self-healing anticorrosion coatings.

2.6.1. Preparation of anticorrosion coatings

Several pieces of steel panel (50 × 50 × 5 mm^3) were firstly polished with sandpaper and then washed with acetone to remove surficial impurities. Subsequently, self-healing resins were coated uniformly on the surface of a steel panel with final thickness of 300–400 μm after cured. After 24 h at room temperature, self-healing specimens were ready for an anticorrosion test. For comparison, specimens covered by pure epoxy resin were prepared as control specimens.

2.6.2. Evaluation of anticorrosion performance

Manual scratches were applied to the specimens followed by immersion in NaCl solutions (1 M) for 24 h for accelerated corrosion. Subsequently, the corrosion performance of self-healing specimens and control specimens were observed. And the detailed information within scratches was observed through SEM.

Besides SEM observation, the self-healing process was also monitored by EIS experiments (Gamry Reference 600 potentiostat) in electrolyte solutions (1 M Sodium Chloride solution). The detailed parameters were listed as following, swept frequency: 10^{-2}-10^5 Hz; and AC amplitude: 20 mV.

3. Results and discussion

3.1. The formation mechanism of the metal shell

The polymer microcapsules (Fig. 1a and as) contained double-layered shell structures (Fig. 1a1, the outer layer of the PUF shell and an inner layer of the polyurea shell), showing outstanding stability in water environments. The synthesis mechanism of polymer microcapsules was discussed in our previous publication [18]. Herein, the growth mechanism of metal shell on the surfaces of polymer microcapsules was explained systematically. The metal shell microcapsules were fabricated by plating chemically a layer of Nickel-P alloy on polymer microcapsules, which were stable enough to avoid the consumption of core material during the plating process. The entire preparation process was divided into two steps. The first step was to deposit Pd particles as a catalyst on the surface of polymer microcapsules, followed by the fabrication of Ni-P alloy in plating solutions.

In order to deposit Pd particles, the Pd suspensions were firstly

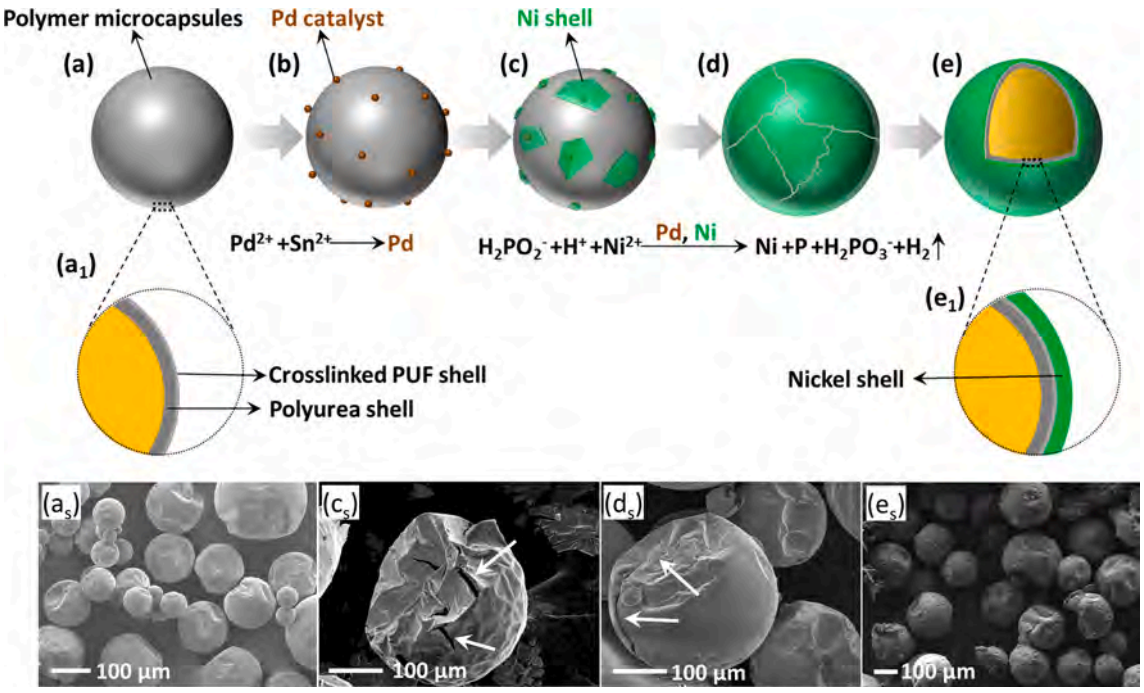

Fig. 1. (a) Polymer microcapsules; (a_1) Double-layered structures of polymer shell; (a_s) Morphology of polymer microcapsules; (b) Polymer microcapsules containing Pd particles on the surfaces; (c) Microcapsules with newly formed Nickel-P shell debris; (c_s) Metal shell microcapsules under plating time of 1 min; (d) Microcapsules with newly formed Nickel-P membranes; (d_s) Metal shell microcapsules under plating time of 5 min; (e) Final metal shell microcapsules, and (e_1) three-layered shell structure of final metal shell microcapsules. (e_s) Metal shell microcapsules under plating time of 60 min.

prepared by reacting $PdCl_2$ with $SnCl_2$ in acid environments. When $SnCl_2$ was added in $PdCl_2$ aqueous solutions, the Pd^{2+} cations were reduced rapidly into suspended nano Pd particles, which were then absorbed on the surface of polymer microcapsules through interfacial interaction (Fig. 1b).

In plating solutions, the Ni^{2+} cations in solutions were reduced immediately by sodium hypophosphite under the activation of Pd catalyst, with the formation of Nickel-P shell debris surrounding Pd particles (Fig. 1c). When plating time was 1 min, the morphology of metal shell microcapsules was incomplete and some holes could be observed (Fig. 1cs). The freshly formed metal Nickel replaced Pd particles as a new catalyst to keep the growth of Nickel-P shell along the tangent of microcapsules surfaces until encountering another piece of increasing shell layer (Fig. 1d). When plating time was 5 min, the polymer microcapsules were covered by a layer of metal shell, and some scars could be observed on the metal shell microcapsules (Fig. 1ds). The metal shell was thickening simultaneously while expanding on the surface of the microcapsule. After complete coverage of microcapsules, the metal shell thickness continued to increase over durations (Fig. 1e and es). The surfactant in the plating solution was applied to eliminate the generated hydrogen bubbles on the shell surface for denser Nickel-P shell. After a certain duration, the metal shell microcapsules were prepared successfully, showed three-layered shell structures (Fig. 1e1).

3.2. Morphology of metal shell microcapsules

The morphologies of metal shell microcapsules were shown in Fig. 2. Fig. 2a showed the overview of well-dispersed metal shell microcapsules with diameters of 184.3 ± 41.7 μm and related size distribution. Some small bumps (Fig. 2b) were observed on the surface of the individual microcapsule, and they were mainly produced from the uneven growth of the Nickel-P shell. The hollow inner structure (Fig. 2c) of microcapsules illustrated that the HMDI core was hardly consumed by the plating solutions, due to the outstanding impermeability of polymer microcapsules. Moreover, the detailed information of cross-sectioned shells was

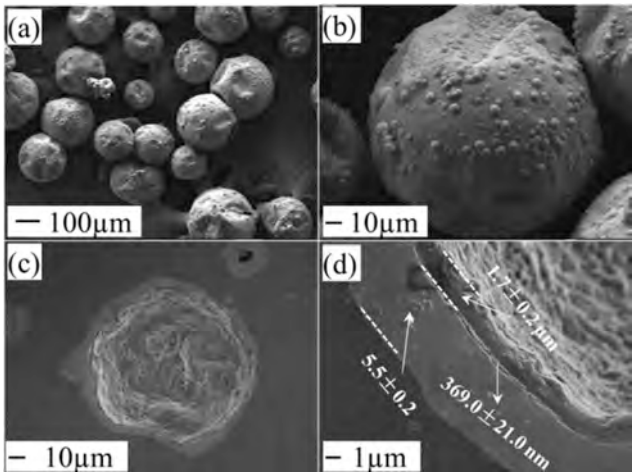

Fig. 2. (a) Overview of metal shell microcapsules; (b) Morphology of single metal shell microcapsules; (c) Metal shell microcapsules showed hollow inner structure; (d) The three-layered shell structure of metal shell microcapsules.

shown in Fig. 2d. The microcapsule shell with a total thickness of 7.4 ± 0.4 μm was a three-layered structure, which comprised of an outer-layered metal shell with a thickness of 5.5 ± 0.2 μm, a medium-layered PUF shell with a thickness of 369.0 ± 21.0 nm, and an inner-layered polyurea shell with a thickness of 1.7 ± 0.2 μm.

Moreover, the outer-layered shell was mainly composed of Nickel-P alloy, whose chemical composition was determined through EDX analysis, as shown in Fig. 3. The specific area on the cross-section area of the metal shell was chosen as the target area (Fig. 3a). The spectra curves of this area showed the existence of Nickel element (89.43 wt%) and Phosphorus element (10.57 wt%) (Fig. 3b and c).

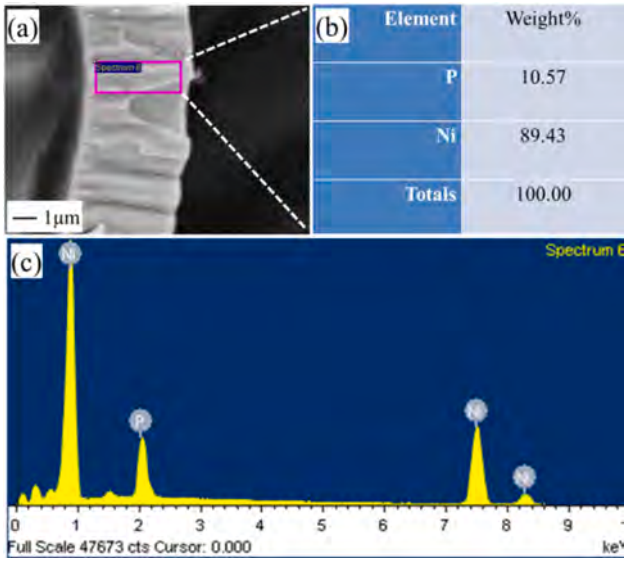

Fig. 3. (a) The test area of a metal shell; (b) Elements composition of metal shell, and (c) EDX spectrum of a metal shell.

3.3. FT-IR characterization of core material

The chemical composition of the core material was determined by comparing the FTIR spectra curves of the core material with that of pure HMDI, as shown in Fig. 4. The nearly identical curves of both substances meant that HMDI was encapsulated successfully. Besides, the characteristic peak of NCO functional groups was presented in 2250 cm^{-1}.

3.4. Core fraction and thermal stability of metal shell microcapsules

The core fraction of metal shell microcapsules was determined by the titration method according to ASTM D2572-97, and then the obtained NCO contents were converted into HMDI fraction as core fraction of metal shell microcapsules. The weight percentage of core materials was 22.4 ± 0.6 wt%, corresponding to the volume percentage of 73.1 ± 1.9%, which was in agreement with the theoretical value. The obvious difference between weight percentage and volume percentage was due to the higher density of Nickel-P alloy (8.9 g/cm^3) than HMDI (1.07 g/cm^3).

The thermal stability was tested by heating metal shell microcapsules, shell material, and pure HMDI from room temperature to 600 °C at a rate of 10 °C min^{-1} in a Nitrogen atmosphere. The residual sample weight as a function of temperature was shown in Fig. 4b.

The shell materials remained nearly constant weight from room temperature to 250 °C, followed by the drop of TGA curves due to the thermal decomposition of organic constituents in shell material, leaving a metallic residue of around 93.0 wt% after 600 °C. The metal shell microcapsules began to lose weight at around 180 °C due to the evaporation of HMDI core, followed by the decomposition of organic parts in the shell layer until 600 °C, leaving nearly 66.0 wt% residue of the pure metal shell. Pure HMDI began to lose weight of 5.0 wt% at around 180 °C followed by the nearly vertical drop of sample weight due to massive evaporation. Microcapsules shell displayed outstanding thermal stability due to the constant weight until 250 °C. The metal shell occupied around 66.0 wt% of final microcapsules providing great potential to improve microcapsules' mechanical property.

3.5. Chemical stability of final microcapsules

The stability of metal shell microcapsules in both organic solvents and water was measured by immersing microcapsules in water and organic solvents for certain durations, followed by the characterization in terms of residual core fractions and morphologies.

3.5.1. Stability of microcapsules in organic solvents

The metal shell microcapsules were soaked in ambient hexane, xylene, ethyl acetate, and acetone for 10 days and 20 days, respectively. The residual core fractions of metal shell microcapsules as a function of immersion durations were shown in Fig. 5. Both morphology and inner structure of microcapsules after immersion in hexane (a_1, a_2), xylene (b_1, b_2), ethyl acetate (c_1, c_2), and acetone (d_1, d_2) were shown in Fig. 6, respectively. As shown in Fig. 5, the residual core fractions of metal shell microcapsules decreased from 22.4 ± 0.6 wt% to 22.1 ± 1.0 wt% (10 days) and 22.2 ± 3.0 wt% (20 days) in hexane, to 23.7 ± 1.0 wt% (10 days) and 21.1 ± 1.0 wt% (20 days) in xylene, to 21.4 ± 0.6 wt% (10 days) and 21.5 ± 0.2 wt% (20 days) in ethyl acetate, and to 22.2 ± 0.7 wt% (10 days) along with 19.9 ± 0.7 wt% (20 days) in acetone, respectively.

Obviously, the polarity of organic solvents influenced slightly the stability of metal shell microcapsules. Especially in acetone, the metal shell microcapsules remained highly stable without an obvious decrease in core fractions. However, the isocyanates core encapsulated within polyurethane and PUF shells were leaked massively within one hour in acetone [13,25]. The outstanding stability of microcapsules was due to the impermeable and stable metal shell. The metal shell was hard to be swelled by organic solvents due to the strong metal bonds, retaining core material of microcapsules in high polar organic solvents. However, when polymeric microcapsules were immersed in organic solvents, the

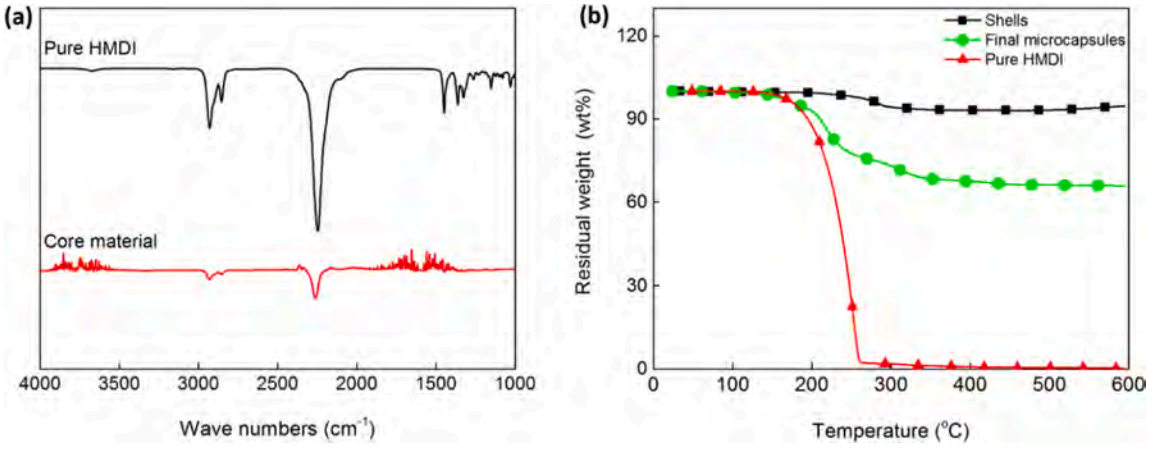

Fig. 4. (a) Comparison of FTIR curves of the core material with pure HMDI; (b) TGA curves of shell material, metal shell microcapsules, and pure HMDI as a function of temperature from room temperature to 600 °C at a rate of 10 °C/min in a Nitrogen atmosphere.

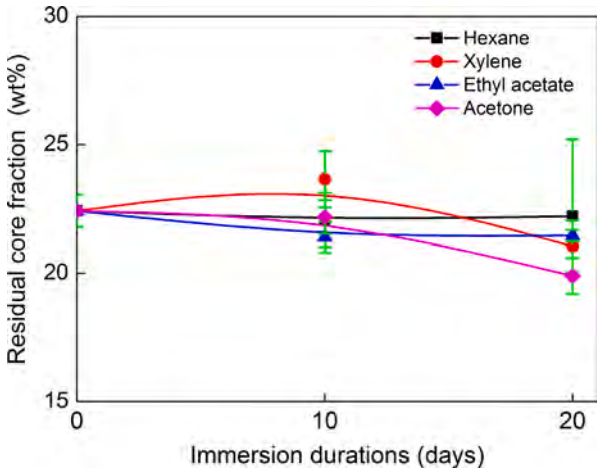

Fig. 5. The residual core fraction of metal shell microcapsules as a function of immersion durations after immersion in hexane, xylene, ethyl acetate, and acetone, respectively.

polymeric shells were swelled seriously resulting in a massive release of core material until osmotic balance [13]. During the swelling process, the mesh size of polymeric shells was enlarged by organic solvents and became more permeable allowing the diffusion-out of the liquid core. By comparison, metal shells showed outstanding stability over traditional polymer shells.

The residual core fractions of metal shell microcapsules fluctuated inconspicuously under longer immersion durations in organic solvents. Even after 20 days, all metal shell microcapsules remained constant morphologies and hollow inner structure, as shown in Fig. 6. Therefore, metal shell microcapsules were available in various harsh environments due to the impermeable and stable metal shells.

3.5.2. Stability of microcapsules in water

The stability of metal shell microcapsules in water affected greatly the service life of anticorrosion coatings, and it was tested by soaking microcapsules in ambient water (ambient temperature was 25 °C) for certain durations, followed by the characterization in terms of residual core fraction and morphologies.

The residual core fractions of metal shell microcapsules as a function of immersion durations in ambient water was shown in Fig. 7a. Fig. 7b_1 and b_2 showed the morphologies and inner structure of metal shell microcapsules after 20 days in ambient water, respectively. The core fractions of metal shell microcapsules decreased from 22.4 ± 0.6 wt% to 21.6 ± 0.2 wt% and 21.0 ± 0.7 wt%, when immersion durations were increased from 0 days to 10 days and 20 days. The residual core fractions of metal shell microcapsules fluctuated slightly with immersion durations, meaning that metal shell microcapsules remained stable in water. Besides, the morphologies of metal shell microcapsules remained spherical morphology (Fig. 7b_1) and hollow inner structure (Fig. 7b_2) after 20 days in ambient water, implying outstanding impermeability of microcapsule shells towards water molecules. By comparing the stability of metal shell microcapsules with that of polymer microcapsules [18], it was reasonable to conclude that metal shell microcapsules possessed good stability in water.

3.6. Mechanical properties of microcapsules and composites

3.6.1. Mechanical properties of single microcapsules

The mechanical properties of metal shell microcapsules were characterized through two parts. The first part was to test the mechanical strength of single metal shell microcapsules through a published method [16]. The second part was to measure the mechanical properties of the epoxy composites containing microcapsules. Polymer microcapsules and metal shell microcapsules were dispersed in epoxy resin at certain concentrations, respectively, and the compressive strength and compressive modulus of epoxy composites were obtained through compression tests.

The micro-compressive apparatus was applied to measure the shell

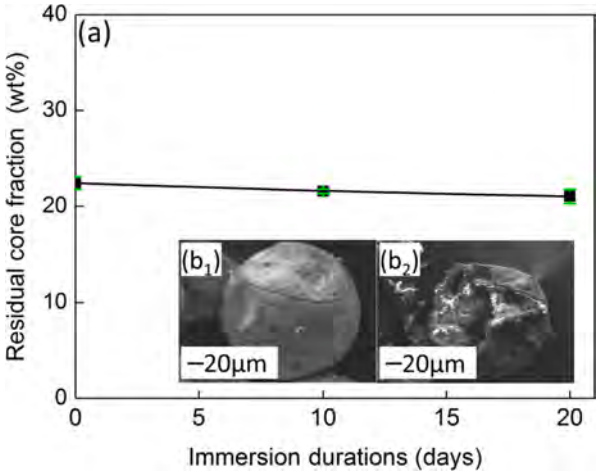

Fig. 7. (a) The residual core fraction of metal shell microcapsules as a function of immersion durations after in ambient water; Both morphology (b_1) and inner structure (b_2) of metal shell microcapsules after immersion in water for 20 days.

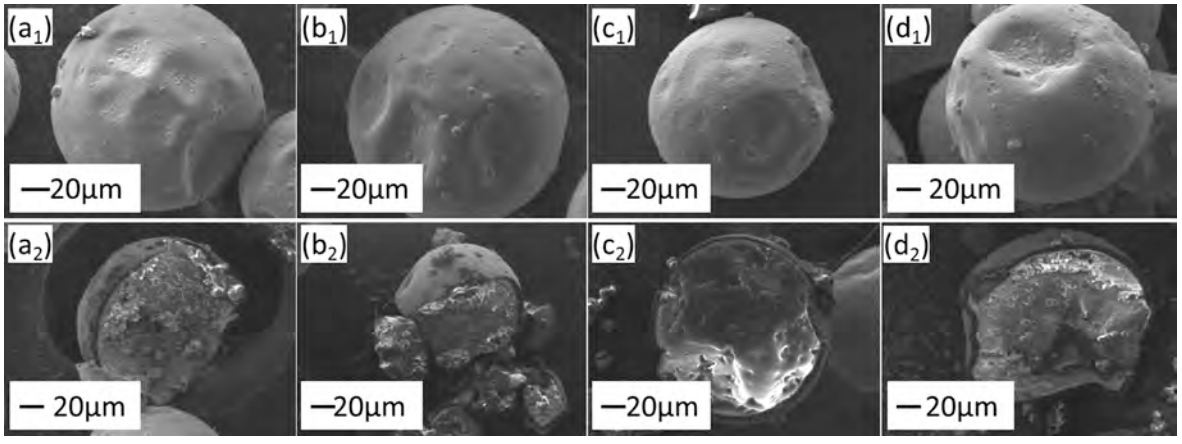

Fig. 6. Both morphologies and hollow structure of metal shell microcapsules after immersion in hexane (a_1, a_2), xylene (b_1, b_2), ethyl acetate (c_1, c_2), and acetone (d_1, d_2), respectively, for 20 days.

strength of polymer microcapsules and metal shell microcapsules according to the published method [16]. Fig. 8a presented the load–displacement curves of polymer microcapsules with diameters of 94.1 μm and metal shell microcapsules with diameters of 99.1 μm.

The corresponding peak load of polymer microcapsule was 7.0 mN, while the peak load of metal shell microcapsules was 45.0 mN. Obviously, metal shell microcapsules possessed a higher peak load than polymer microcapsules.

Also, the normalized shell strength (δ_{max}) of microcapsules was calculated according to a previous publication [26], and the equation was shown in the following:

$$\delta_{max} = \frac{P_{max}}{\pi\left[\left(\frac{D_0}{2}\right)^2 - \left(\frac{D_i}{2}\right)^2\right]} = \frac{P_{max}}{\pi t(D_0 - t)} \quad (4)$$

where P_{max} was the maximum load, D_0 was the outer diameter of microcapsules, D_i was the inner diameter of microcapsules, and t was the shell thickness of microcapsules.

Based on a total of 10 measurements, the statistic shell strengths of polymer microcapsules and metal shell microcapsules were 6.6 ± 2.5 MPa and 28.5 ± 10.3 MPa, respectively, as shown in Fig. 8b. Obviously, the shell strength of microcapsules was improved by 332% by covering a layer of metal shell on polymer microcapsules due to the higher strength and modulus of Ni-P alloy.

3.6.2. Mechanical properties of epoxy composites

Compression test of epoxy composites containing polymer microcapsules and metal shell microcapsules at different concentrations (10.0 wt%, 20.0 wt%, and 30.0 wt%) was conducted according to ASTM-D695, and the mechanical properties of composites were characterized in terms of compression strength and modulus, as shown in Fig. 9a and b.

As shown in Fig. 9a, the epoxy composites showed weaker compression strength with the increase of microcapsules concentrations. The compressive strength of polymer microcapsules based composites decreased from 101.0 ± 1.4 MPa to 72.2 ± 0.1 MPa, 55.0 ± 0.2 MPa, and 40.3 ± 0.0 MPa corresponding to the microcapsules concentrations of 0.0 wt%, 10.0 wt%, 20.0 wt%, and 30.0 wt%, respectively. For comparison, the compressive strength of metal shell microcapsules based composites decreased from 101.0 ± 1.4 MPa to 86.9 ± 0.7 MPa, 78.2 ± 0.4 MPa, and 69.4 ± 1.1 MPa under the corresponding microcapsules concentrations. The compressive strength of both composites showed a decreasing trend with the increase of microcapsules concentrations. The microcapsules in epoxy composites were considered as a kind of flaws, and higher microcapsule concentrations brought more flaws and therein more focal point of stress, resulting in weaker compressive strength. Although the compressive strength of both epoxy composites showed decreasing trends under higher microcapsules concentrations, epoxy composites containing metal shell microcapsules still possessed higher compressive strength than that containing polymer microcapsules. The difference was magnified significantly under higher microcapsules concentrations. The main reason was that the metal shell possessed higher mechanical strength than polymer shells.

Different from compressive strength, the compressive modulus of epoxy composites varied slightly with the concentrations of metal shell microcapsules. However, the compressive modulus of epoxy composites containing polymer microcapsules remained in a decreasing trend. As shown in Fig. 9b, the modulus of epoxy composites containing polymer microcapsules decreased from 2.5 ± 0.1 GPa, to 2.2 ± 0.1 GPa, 1.8 ± 0.0 GPa, and 1.2 ± 0.0 GPa corresponding to the increase of microcapsules concentration from 0.0 wt% to 10.0 wt%, 20.0 wt%, and 30.0 wt%, respectively. When metal shell microcapsules were introduced in an epoxy matrix, the modulus of composites remained stable relatively around 2.5 ± 0.1 GPa, 2.5 ± 0.0 GPa, 2.5 ± 0.0 GPa, and 2.4 ± 0.0 GPa with the increase of microcapsules concentration from 0.0 wt% to 10.0 wt%, 20.0 wt%, and 30.0 wt%, respectively. The main reason was that the metal shell possessed nearly identical modulus with epoxy matrix [23]. The higher modulus of epoxy composites containing metal shell microcapsules than those containing polymer microcapsules was due to the higher modulus of metal shell microcapsules.

3.7. Anticorrosion performance of self-healing composites

In order to investigate anticorrosion performance, metal shell microcapsules were dispersed in epoxy resin at a concentration of 10.0 v%, and then coated uniformly on steel panels through spreader (KTQ-II) as self-healing specimens with a final thickness of 300–400 μm after cure. The thickness of the fresh coating was controlled by adjusting the distance between spreader blades and the steel panel surfaces. The cured coating thickness was tested through a thickness gauge based on at least 10 positions. Besides, control samples covered by pure epoxy resin were also prepared for comparison.

After curing for 24 h at ambient temperature, manual scratches were applied to all specimens, which were then immersed in salty water (NaCl 1 M) for accelerated corrosion. After 24 h, the corrosion performances of specimens were shown in Fig. 10. As shown in Fig. 10a, severe corrosion occurred to control samples because of empty scratches (Fig. 10b) resulting in the direct exposure of steel substrates in corrosive environments. In comparison, self-healing samples containing metal shell microcapsules (Fig. 10c) were fully rust-free after 24 h immersion in corrosive environments. The main reason was that the released HMDI from broken microcapsules sealed the scratches, by polymerizing with ambient moisture into the polyurea membrane, as shown in Fig. 10d. The polyurea films within scratches isolated efficiently ambient

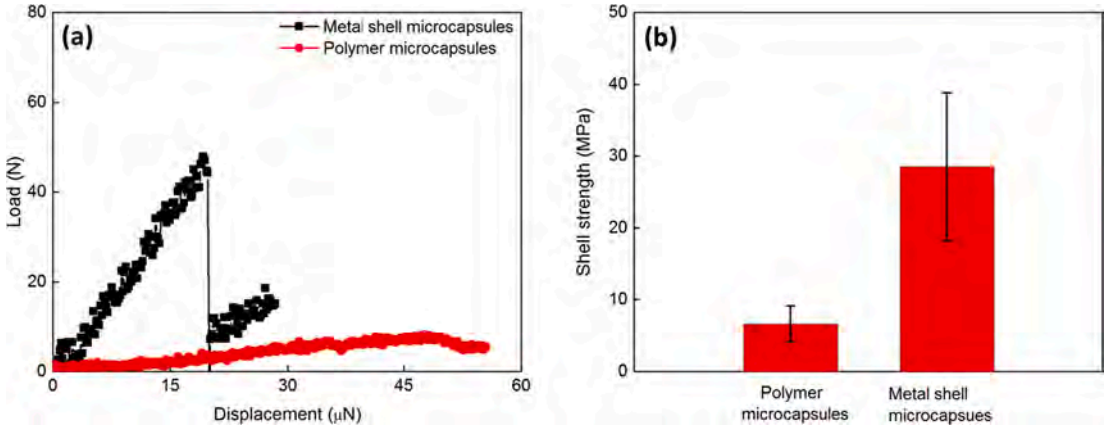

Fig. 8. (a) Typical load-displacement curves of polymer microcapsules and metal shell microcapsules; (b) Normalized shell strength of polymer microcapsules and metal shell microcapsules.

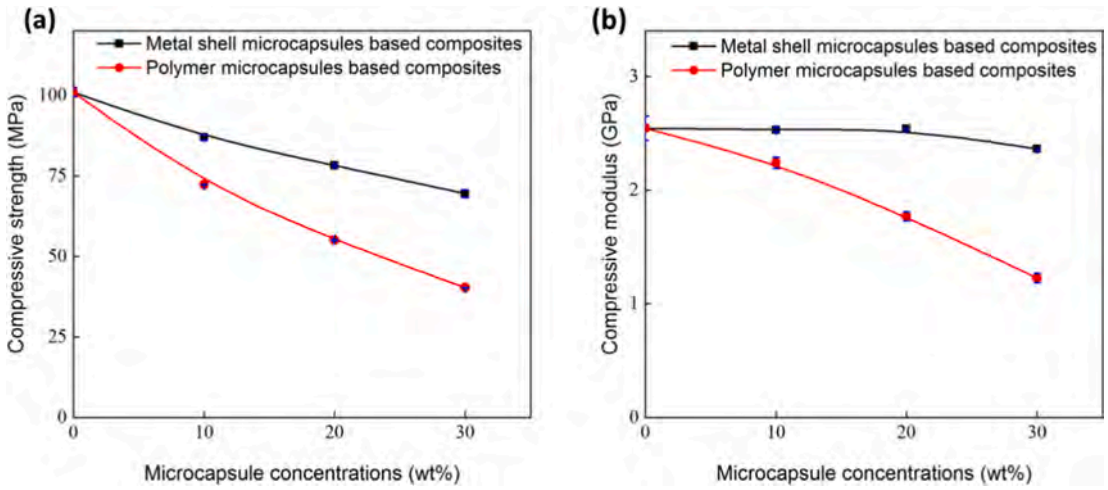

Fig. 9. Compressive strength (a) and compressive modulus (b) of epoxy composites containing polymer microcapsules and metal shell microcapsules as a function of microcapsules concentration.

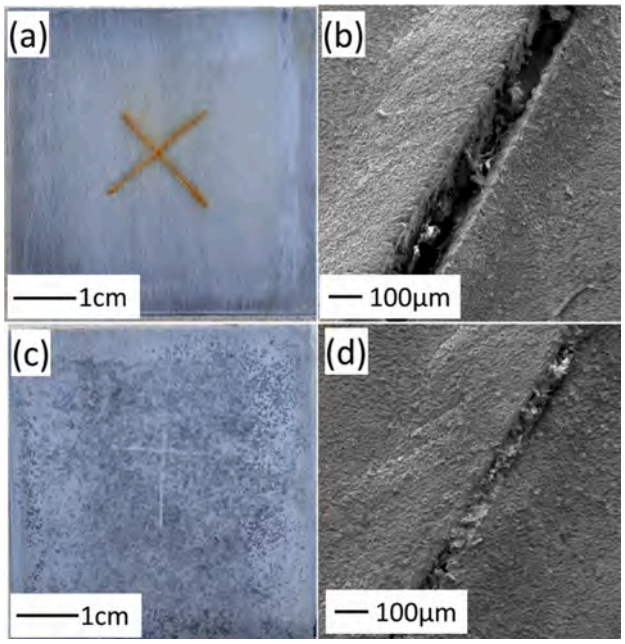

Fig. 10. The corrosion performances and detailed scratch information of coatings including neat epoxy coating (a, b), and self-healing coatings containing metal shell microcapsules (c, d).

moisture to keep the steel substrates free of rust.

3.8. EIS investigation of the self-healing process

The anticorrosion processes of self-healing specimens were further characterized through Electrochemical Impedance Spectroscopy (EIS) based on the published model (Fig. 11a) and equivalent circuit (Fig. 11c) [27]. The obtained healing resistance ($R_{healing}$) from equivalent circuits supplied particular information about the self-healing process at the scratched area. Fig. 11b showed the schematic model of the self-healing phenomenon within cracks. When cracks occurred to self-healing coatings, the microcapsules were broken and released liquid healing agents to seal the cracks. The microcapsules were located on the surface of steel panels due to the high density of metal shell, and this phenomenon allowed the hardness and modulus of the coating surfaces were highly similar with pure epoxy coating, avoiding the decrease of coating modulus with the introduction of microcapsules.

Fig. 11d presented the $R_{healing}$ of self-healing coating varied with corrosion durations. As shown in Fig. 11d, the $R_{healing}$ of self-healing coatings containing metal shell microcapsules rose from 261.4 Ω to 1.9×10^4 Ω and 5.5×10^4 Ω when immersion duration in NaCl solutions extended from 1 h to 4 h, and 24 h, respectively. The higher $R_{healing}$ under longer immersion time meant that more healing agent was polymerized in the scratched area increasing electrical resistance of coatings.

4. Conclusion

Metal shell microcapsules containing HMDI as core material were synthesized successfully. The achieved progress was presented as follows:

(1) The metal shell microcapsules with a diameter of 184.3 ± 41.7 μm and shell thickness of 7.4 ± 0.4 μm contained 22.4 ± 0.6 wt% of HMDI as core material.
(2) The metal shell microcapsules possessed outstanding impermeability and stability in low polar organic solvents, high polar organic solvents, and water. Besides, the final microcapsules possessed higher mechanical strength than polymer microcapsules. Although epoxy composites showed decreasing mechanical strength with metal shell microcapsule concentrations, the modulus of the composite remained stable relatively, implying good resistance to environmental physical damages.
(3) Most importantly, metal shell microcapsules still showed good self-healing anticorrosion performance in epoxy coatings through accelerated corrosion experiments and the EIS test.

CRediT authorship contribution statement

Dawei Sun: Methodology, Investigation, Writing - original draft, Writing - review & editing. **Zheng Yan:** Project administration, Formal analysis. **Lan Mingzhang:** Supervision, Formal analysis. **Wang Ziming:** Supervision, Formal analysis. **Cui Suping:** Resources, Supervision, Formal analysis, Funding acquisition, Writing - review & editing. **Yang Jinglei:** Conceptualization, Resources, Formal analysis, Funding acquisition.

Declaration of Competing Interest

The authors declare that they have no known competing financial

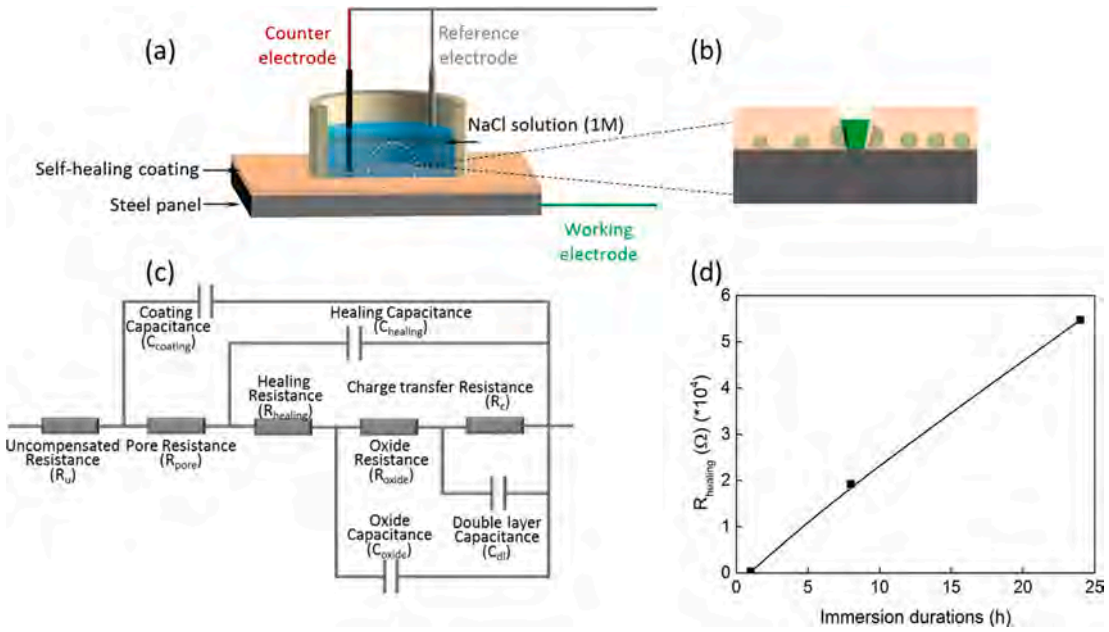

Fig. 11. The schematic picture of EIS experiment model (a) and self-healing results of coating cracks (b); The equivalent circuit was applied to obtain the healing resistance of scratched coatings ($R_{healing}$) by curve fitting (c); The healing resistance ($R_{healing}$) of scratched self-healing coating as a function of immersion durations (d).

interests or personal relationships that could have appeared to influence the work reported in this paper.

Acknowledgements

Support from Beijing Natural Science Foundation under grant (2194069), General Program of Science and Technology Development Project of Beijing Municipal Education Commission (KM202010005004), and the National Natural Science Foundation of China (52002006) are gratefully acknowledged.

Data availability

All data, models, and code generated or used during the study appear in the submitted article.

References

[1] H.-S. Ryu, J.K. Singh, H.-S. Lee, M.A. Ismail, W.-J. Park, Effect of $LiNO_2$ inhibitor on corrosion characteristics of steel rebar in saturated $Ca(OH)_2$ solution containing NaCl: an electrochemical study, Constr. Build. Mater. 133 (2017) 387–396.
[2] A. Goyal, H.S. Pouya, E. Ganjian, P. Claisse, A review of corrosion and protection of steel in concrete, Arab. J. Sci. Eng. 43 (2018) 5035–5055.
[3] A. James, E. Bazarchi, A.A. Chiniforush, P. Panjebashi Aghdam, M.R. Hosseini, A. Akbarnezhad, I. Martek, F. Ghodoosi, Rebar corrosion detection, protection, and rehabilitation of reinforced concrete structures in coastal environments: a review, Constr. Build. Mater. 224 (2019) 1026–1039.
[4] H. DorMohammadi, Q. Pang, P. Murkute, L. Árnadóttir, O.B. Isgor, Investigation of chloride-induced depassivation of iron in alkaline media by reactive force field molecular dynamics, npj Mater. Degrad. 3 (2019) 19.
[5] W. Funke, How organic coating systems protect against corrosion, in: Polymeric Materials for Corrosion Control, American Chemical Society, 1986, pp. 222–228.
[6] S.H. Cho, S.R. White, P.V. Braun, Self-healing polymer coatings, Adv. Mater. 21 (2009) 645–649.
[7] Y. Zhao, W. Zhang, L.-P. Liao, S.-J. Wang, W.-J. Li, Self-healing coatings containing microcapsule, Appl. Surf. Sci. 258 (2012) 1915–1918.
[8] A.C. Jackson, J.A. Bartelt, K. Marczewski, N.R. Sottos, P.V. Braun, Silica-protected micron and sub-micron capsules and particles for self-healing at the microscale, Macromol. Rapid Commun. 32 (2011) 82–87.
[9] M. Huang, J. Yang, Facile microencapsulation of HDI for self-healing anticorrosion coatings, J. Mater. Chem. 21 (2011) 11123–11130.
[10] M. Huang, H. Zhang, J. Yang, Synthesis of organic silane microcapsules for self-healing corrosion resistant polymer coatings, Corros. Sci. 65 (2012) 561–566.
[11] R.S. Jadhav, D.G. Hundiwale, P.P. Mahulikar, Synthesis and characterization of phenol–formaldehyde microcapsules containing linseed oil and its use in epoxy for self-healing and anticorrosive coating, J. Appl. Polym. Sci. 119 (2011) 2911–2916.
[12] D. Zhao, S. Liu, Y. Wu, T. Guan, N. Sun, B. Ren, Self-healing UV light-curable resins containing disulfide group: synthesis and application in UV coatings, Prog. Org. Coat. 133 (2019) 289–298.
[13] D. Sun, J. An, G. Wu, J. Yang, Double-layered reactive microcapsules with excellent thermal and non-polar solvents resistance for self-healing coatings, J. Mater. Chem. A 3 (2015) 4435–4444.
[14] W. Wang, L.K. Xu, F. Liu, X.B. Li, L.K. Xing, Synthesis of isocyanate microcapsules and micromechanical behavior improvement of microcapsule shells by oxygen plasma treated carbon nanotubes, J. Mater. Chem. A 1 (2013) 776–782.
[15] M.M. Caruso, B.J. Blaiszik, H.H. Jin, S.R. Schelkopf, D.S. Stradley, N.R. Sottos, S. R. White, J.S. Moore, Robust, double-walled microcapsules for self-healing polymeric materials, Acs Appl. Mater. Inter. 2 (2010) 1195–1199.
[16] H. Zhang, P. Wang, J. Yang, Self-healing epoxy via epoxy–amine chemistry in dual hollow glass bubbles, Compos. Sci. Technol. 94 (2014) 23–29.
[17] D. Sun, H. Zhang, X.-Z. Tang, J. Yang, Water resistant reactive microcapsules for self-healing coatings in Harsh environments, Polymer 91 (2016) 33–40.
[18] D. Sun, Y.B. Chong, K. Chen, J. Yang, Chemically and thermally stable isocyanate microcapsules having good self-healing and self-lubricating performances, Chem. Eng. J. 346 (2018) 289–297.
[19] J.D. Affinito, M.E. Gross, C.A. Coronado, G.L. Graff, I.N. Greenwell, P.M. Martin, A new method for fabricating transparent barrier layers, Thin Solid Films 290 (1996) 63–67.
[20] V.N. Talash, V.A. Lavrenko, O.A. Frenkel, Preparation and properties of iron powder plated with nickel and cobalt, Powder Metall. Met. Cer. 41 (2002) 342–346.
[21] H.J. Zhang, Y. Liu, Preparation and microwave properties of Ni hollow fiber by electroless plating-template method, J. Alloy. Compd. 458 (2008) 588–594.
[22] M.W. Patchan, L.M. Baird, Y.-R. Rhim, E.D. LaBarre, A.J. Maisano, R.M. Deacon, Z. Xia, J.J. Benkoski, Liquid-filled metal microcapsules, Acs Appl. Mater. Inter 4 (2012) 2406–2412.
[23] D. Sun, H. Zhang, X. Zhang, J. Yang, Robust metallic microcapsules: a direct path to new multifunctional materials, Acs Appl. Mater. Inter. 11 (2019) 9621–9628.
[24] M.K.K.N.R. Sottos, Mechanical properties of microcapsules used in a self-healing polymer, Exp. Mech. 46 (2006) 725–733.
[25] G. Wu, J. An, X.Z. Tang, Y. Xiang, J. Yang, A versatile approach towards multifunctional robust microcapsules with tunable, restorable, and solvent-proof superhydrophobicity for self-healing and self-cleaning coatings, Adv. Funct. Mater. 24 (2014) 6751–6761.
[26] J.L. Yang, M.W. Keller, J.S. Moore, S.R. White, N.R. Sottos, Microencapsulation of Isocyanates for Self-Healing Polymers, Macromolecules 41 (2008) 9650–9655.
[27] M. Huang, J. Yang, Salt spray and EIS studies on HDI microcapsule-based self-healing anticorrosive coatings, Prog. Org. Coat. 77 (2014) 168–175.